

# REPORT DOCUMENTATION PAGE

AFRL-SR-AR-TR-04-

Public reporting burden for this collection of information is estimated to average 1 hour per response, including the time for reviewing instructions, gathering existing data needed, and completing and reviewing this collection of information. Send comments regarding this burden estimate or any other aspect of this burden to Department of Defense, Washington Headquarters Services, Directorate for Information Operations and Reports (0704-0188), 4302. Respondents should be aware that notwithstanding any other provision of law, no person shall be subject to any penalty for failing to comply with a collection of information if it does not have a valid OMB control number. PLEASE DO NOT RETURN YOUR FORM TO THE ABOVE ADDRESS.

0551

1. REPORT DATE (DD-MM-YYYY) 20-10-2004		2. REPORT TYPE Final Report		3. DATES COVERED (From - To) 01-09-2001 to 01-09-2004	
4. TITLE AND SUBTITLE <del>AFOOR Cylindrical Vircator Optimization Project</del>				5a. CONTRACT NUMBER 1303-44-1465	
				5b. GRANT NUMBER 01-1-0537	
				5c. PROGRAM ELEMENT NUMBER	
6. AUTHOR(S) M. Kristiansen and J. Mankowski				5d. PROJECT NUMBER	
				5e. TASK NUMBER	
				5f. WORK UNIT NUMBER	
7. PERFORMING ORGANIZATION NAME(S) AND ADDRESS(ES) Texas Tech University Center for Pulsed Power and Power Electronics Dept of Electrical Engineering Lubbock, TX 79409				8. PERFORMING ORGANIZATION REPORT NUMBER	
9. SPONSORING / MONITORING AGENCY NAME(S) AND ADDRESS(ES) AFOSR  NE				10. SPONSOR/MONITOR'S ACRONYM(S)	
				11. SPONSOR/MONITOR'S REPORT NUMBER(S)	
12. DISTRIBUTION / AVAILABILITY STATEMENT Distribution Statement A: unlimited					
13. SUPPLEMENTARY NOTES					
14. ABSTRACT Traditionally, the radiated microwave frequency in a coaxial vircator is considered to be determined primarily by the virtual cathode oscillation frequency and the electron reflection frequency. In this paper, some experiments showing different results are reported. Particularly, the E-beam is observed to play an important role in the cavity formation. Some possible explanations, including a virtual cavity concept, are proposed. The cavity resonance effect on a coaxial virtual cathode oscillator with different geometries has been investigated in detail. Investigation of the E-beam performance will improve understanding of the interaction between the E-beam and microwaves, which is key for determining the microwave frequency. These results are helpful in optimizing the design of a cylindrical diode to avoid microwave frequency shifting and mode competition.					
15. SUBJECT TERMS					
16. SECURITY CLASSIFICATION OF:			17. LIMITATION OF ABSTRACT	18. NUMBER OF PAGES 9	19a. NAME OF RESPONSIBLE PERSON John Mankowski
a. REPORT	b. ABSTRACT	c. THIS PAGE			19b. TELEPHONE NUMBER (include area code) (806) 742-0526

Standard Form 298 (Rev. 8-98)  
Issued by ANSI Std. Z39.18

20041105 141

# Final Report on Coaxial Virtual Cathode Enhancement

Center for Pulsed Power and Power Electronics  
Texas Tech University

## I. Introduction

The following is a report on a series of experimental tests to increase the power and efficiency of the Texas Tech Coaxial Virtual Cathode oscillator (Vircator). The tests were aimed at increasing the efficiency by modifying the geometry of the Vircator cavity. It is believed that resonances are established in the cavity that

- increase output power of the microwaves and
- assist in pre-modulating the E-beam.

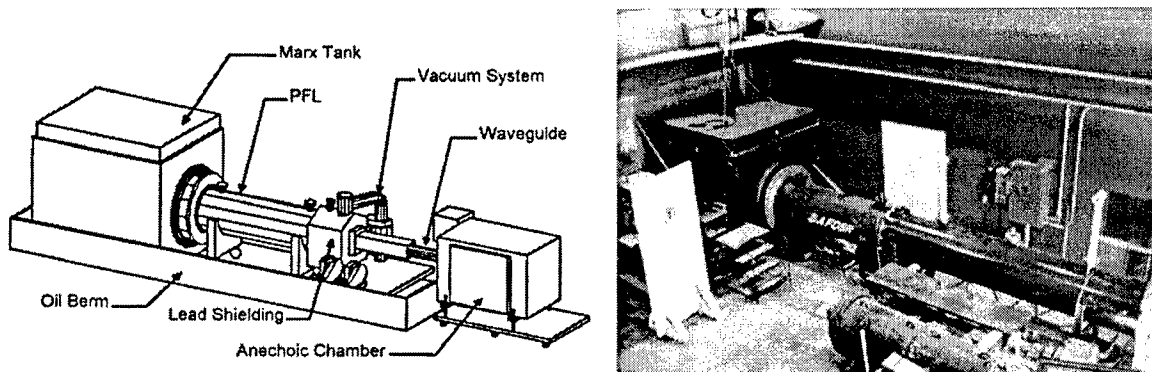


Figure 1. Schematic and image of the Marx-bank PFL assembly.

## II. Experimental Setup

A schematic and image of the Marx-bank and PFL assembly used to drive the Vircator is shown in Figure 1 above. Typical output to the Vircator diode is  $\sim -600$  kV, 70 kA, for 100 nsec. A voltage and current waveform to the diode is shown in Figure 2.

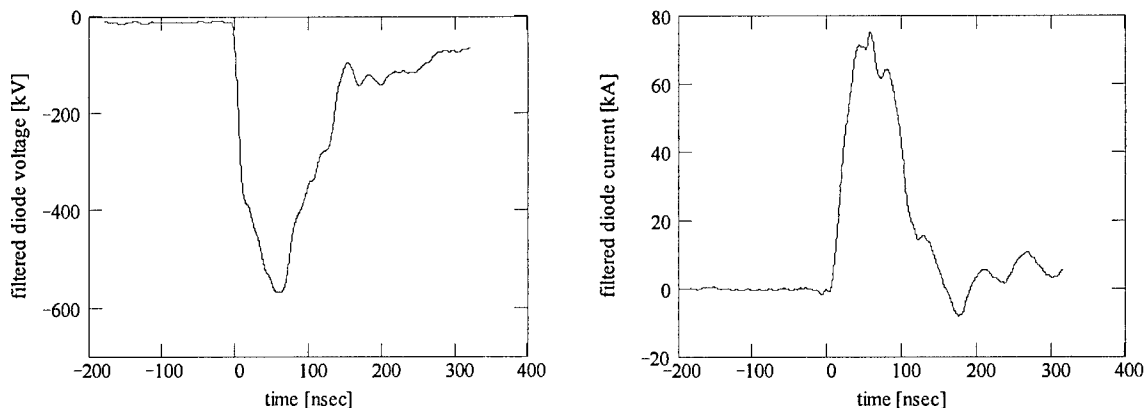
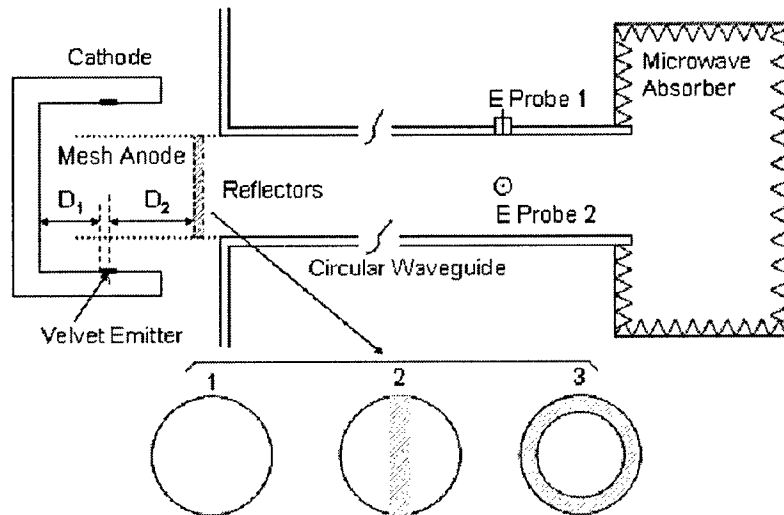


Figure 2. Typical output waveforms to the Vircator diode.

The core of the experimental configuration is the coaxial diode. The aluminum cathode is connected to the output of the pulse generator and the stainless mesh anode is grounded to the aluminum waveguide. The cathode has a velvet strip with a width of 3.5 cm working as an explosive emitter. Electrons from the emitter can pass through the mesh anode to enter the inner anode region, where the virtual cathode forms and oscillates. The cathode radius is 13.1 cm and the anode radius is 9.9

cm. The waveguide radius is 9.8 cm, close to that of the anode. The 2.5 m long waveguide is connected to the mesh anode at one end and to the microwave absorber at the other end. Two E-probes are installed in the waveguide wall, 1.5 m from the anode end,  $90^\circ$  apart on the azimuth, so that one is referred to the horizontal probe and the other as the vertical probe.

To investigate the resonance effect in the cylindrical diode, we changed the emitter position,  $D_1$ , to 4 cm, 5.08 cm, 6 cm and 7 cm from the cathode back wall. For a certain emitter position, we used three different reflector arrangements near the waveguide: no reflector (1), a strip reflector (2), or a donut reflector (3) as shown in Figure 3. The reflectors are made of copper plate. The strip reflector has a width of 2.56 cm and the donut reflector has an inner radius of 8 cm and outer radius of 9.8 cm. The reflector position,  $D_2$ , relative to the cathode emitter is also changed. For any fixed geometry sharing the same emitter width, emitter position, reflector type and reflector position, we vary the pulse voltage over a range. For a different velvet emitter width of 1 cm, we change  $D_1$ ,  $D_2$  and the applied pulse voltage and get another set of data.



**Figure 3. Experimental configuration, showing the diode, the waveguide and the absorber. Three reflector designs are shown**

Two high-frequency cables carry the two E-probe signals to oscilloscopes in a screen room. The cables are calibrated by a TDR and a HP8719C network analyzer. We use the TDR to make sure that the electrical lengths of the two cables are the same, within 20 ps. The network analyzer is used to calibrate the attenuation of the two cables. We use two oscilloscopes to sample the E-probe signals, an Agilent Infiniium oscilloscope with 2.25GHz bandwidth, 8 GS/s sampling rate and a Tektronix TDS6604 with 6GHz bandwidth and a 20GS/s sampling rate. This configuration was also used to study the power efficiency in earlier investigations. What we do now is to use faster oscilloscopes to monitor the raw signals from the E-probes.

In addition, we have a capacitive probe, a B-dot probe and a Rogowski coil to monitor the diode voltage and diode current, respectively. Since we are most concerned with the microwave frequency, we obtain these diode voltage and current signals just for reference.

### III. Experimental Results

We get the microwave frequency by applying a fast Fourier transformation (FFT) to the microwaves detected by the two E-probes. Figure 3 shows typical horizontal and vertical probe signals for the same shot. Figure 5 shows the frequency spectrum from figure 4. From figure 5, we can see that the peak frequencies of the horizontal and vertical probe signals are slight different, however, their

bandwidths overlap considerably. Within the accuracy of our measurement, we consider the frequencies of the horizontal and vertical probe signals for the same shot to be the same with the same bandwidth. Based on the results after we apply a series of digital band-pass filters to the microwaves detected by the two E-probes, we found that the microwaves at different frequencies occur at the same time and not a result of chirping.

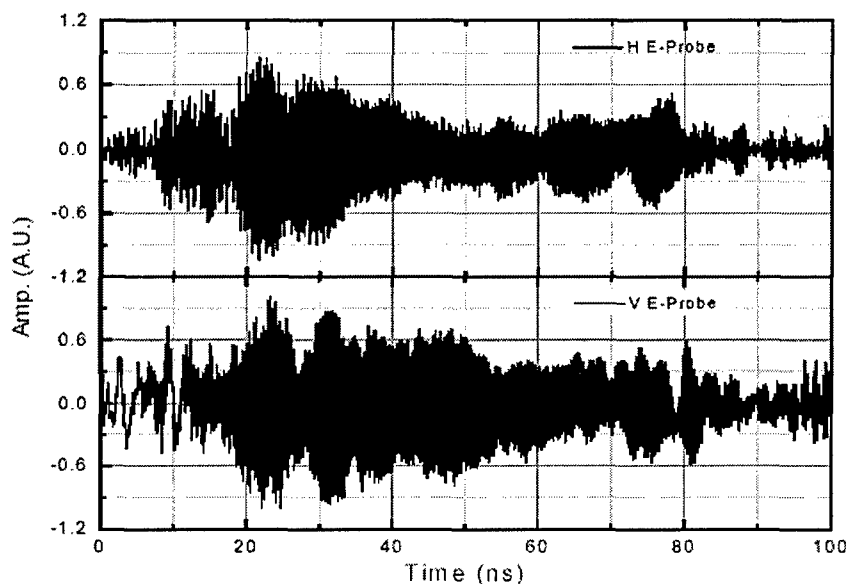


**Figure 4. Waveforms directly obtained by the two E-probes: 0-100 ns.**

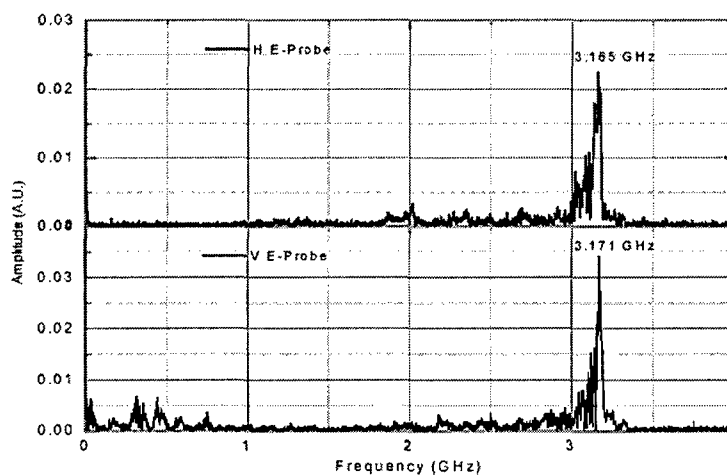


**Figure 5. Frequency spectrum (FFT) of the waveforms shown in Fig. 4.**

Table 1 is typical frequency information for some shots. Generally the first column, shot number, represents the charging voltage of two back-to-back capacitors in the Marx generators and has some relation to the diode voltage. Columns two to five are FFT results for the raw horizontal and vertical fields, where the peak frequencies and their corresponding amplitudes are shown. Sometimes, there are two or more peak frequencies shown simultaneously, although table 1 does not show this. In this case, we consider their relative intensities to determine the dominant peak frequency and the secondary peak frequency. Columns six and seven represent the measured diode voltage and current, where we can see the relative magnitudes of the applied voltage and diode current.

**Table 1. Typical experimental records for certain diode geometry, showing peak frequencies for the two E-probes, their relative magnitudes and the relative diode applied**

## voltage and current.

Shot No.	H Probe Peaks		V Probe Peaks		Diode V-I	
	Freq. (GHz)	Amp. (A.U.)	Freq. (GHz)	Amp. (A.U.)	V. (A.U.)	I. (A.U.)
Shot 60	3.06	3.74	3.06	12.8	2.55	1.27
Shot 62	3.08	3.17	3.07	6.60	2.56	1.26
Shot 64	3.09	2.47	3.09	5.95	2.47	1.36
Shot 66	3.07	2.50	3.06	8.75	2.52	1.30
Shot 68	3.14	2.33	3.14	7.30	2.58	1.48
Shot 70	3.16	4.49	3.17	6.81	2.62	1.53
Shot 72	3.16	4.19	3.16	6.04	2.61	1.75
Shot 74	3.18	4.53	3.17	6.88	2.66	1.61
Shot 76	3.16	5.28	3.17	4.36	2.67	1.95
Shot 78	3.16	8.12	3.17	5.06	2.75	1.67

For all these shots in table 1, the diode physical structures are the same. We vary the charging voltage, resulting in a diode voltage and current change. In table 1, we can see that the microwave frequency increases slightly with the diode voltage or current, which is predicted by the frequency dependence on the electron plasma density [1]. For our research on the cavity effect, we will consider these frequencies as a single frequency for simplicity. For the geometry in table 1, we consider the microwave frequency as 3.16 GHz or so. Not all of our experimental data looks as neat as table 1. In some diode geometries, with a diode voltage or current change, the microwave frequency will “jump” from one band to another band. In this case, we will choose one dominant peak frequency depending on the reflector type.

Based on the explanation above, we will list two dominant peak frequencies for every coaxial diode structure. We will list the frequency for those diode structures in three tables: the first for structures without any reflector, the second for structures with a donut reflector and the third for structures with a strip reflector.

## IV. Cavity Resonance Effect and Virtual Cavity

Generally, the virtual cathode oscillator working frequencies are considered to be determined by the electron reflecting frequency and the virtual cathode oscillation frequency. These frequencies depend on the diode gap distance and the applied diode voltage and current [1], [5], [6]. For our experimental vacuum diode with a 500 kV applied pulse, the theoretical prediction frequencies are: virtual cathode oscillation, 1.8- 2.5GHz, electron reflecting frequency, 1.80GHz. Actually, these predictions offer only some design guidance; they are different from the experimental data because different Approximate models ignore different physical effects. We design the diode to make these two frequencies coincident to get maximum microwave power output [7].

Table 2 is a summary list for the diode structure without reflectors. From table 2, we can see that the dominant peak frequencies decrease as the velvet emitter is moved farther from the back wall of the cathode, although the microwave frequencies for 3.5 cm and 1 cm velvet emitters change at different values of  $D_1$ . These results cannot be explained by conventional cavity theory because the geometry illustrated in Fig. 3 without a reflector doesn't form an enclosed structure. Traditionally, the microwave frequencies in a structure with an open end depend only on the microwave source frequencies. Even though some parts of the diode structure form partial enclosed structures, for different  $D_1$ , those structures are fixed and shouldn't cause the output microwave frequency to change with different velvet emitter position. One possible explanation is that a cavity is formed by the collected electrons or Ebeam, the back wall of the cathode and the mesh anode. This is reasonable since the Ebeam itself acts as a conductor. We can call this kind of cavity a virtual cavity

since it has no obvious physical boundary. It is too early to comment on that because, so far, we cannot determine the propagating mode exactly. Although we have some evidence showing possible  $TM_{01}$  and  $TM_{11}$  modes based on the directivity measurement at the open end of the waveguide in another set of experiments, we still need more solid evidence to clarify them.

**Table 2. Frequency list for geometries without reflectors, showing the microwave frequencies based on their relative power for different geometries.**

Cathode width (cm)	$D_1$ (cm)	Dominant peak (GHz)	Secondary peak (GHz)
3.5	4	3.17	1.95
3.5	5.08	3.16	—*
3.5	6	2.70	2.0
3.5	7	2.68	1.95
1	4	3.0	2.10
1	5	3.0	1.85
1	6	2.93	1.82
1	7	2.60	1.90

Let us look at the secondary peaks in table 2. We can see that the secondary peaks have almost the same frequency for different  $D_1$ . This means, the secondary peak frequencies is independent on the virtual cavity mentioned above. This 2.0 GHz band falls within the theoretical predictions: 1.8-2.5 GHz. A reasonable explanation for this phenomenon is that the secondary peak frequency is one of the microwave source frequencies; the virtual cathode oscillation frequency or the electron reflection frequency.

## V. The Functions of the Reflectors

Table 3 is a frequency list with the donut reflector at different positions. From Table 3, we can see that the donut reflector has little influence on the microwave frequency for both 3.5 cm and 1 cm velvet emitter width, which means that the reflection is not strong enough to change the cavity. Although one odd point occurs at  $D_1=6$  cm and  $D_2=3$  cm for 1 cm velvet emitter, the basic tendency is same for both cases. We do observe that the microwave power generally is decreased by the donut reflector.

**Table 3. Frequency list for geometries with a donut reflector, showing the microwave frequencies based on their relative power for different geometries.**

Cathode width (cm)	D1 (cm)	D2 (cm)	Dominant peak (GHz)	Secondary Peak (GHz)
3.5	4	3.08	3.14	2.07
3.5	4	4.08	3.20	2.0
3.5	4	5.08	3.16	2.0
3.5	4	6.08	3.13	2.0
3.5	5.08	3	3.16	-
3.5	5.08	4	3.16	-
3.5	5.08	5	3.16	2.0
3.5	5.08	6	3.16	2.0
3.5	6	3.08	2.70	-
3.5	6	4.08	2.68	2.05
3.5	6	5.08	2.70	2.0
3.5	6	6.08	2.76	2.0
1	4	3	2.90	1.40
1	4	4	2.90	1.36
1	4	5	2.90	2.07
1	4	6	2.90	2.60
1	5	3	3.0	1.85
1	5	4	3.0	1.82
1	5	5	2.95	-
1	5	6	3.0	-
1	6	3	3.60	2.70
1	6	4	2.93	3.66
1	6	5	2.90	-
1	6	6	2.86	-

Table 4 is a frequency list for the strip reflector at different positions. From Table 4, we can see that the strip reflector changes the microwave dominant frequency for the 3.5 cm velvet cathode from 3.16 GHz in geometries without reflectors to 2.0 GHz. However, the dominant microwave frequency with the 3.5 cm velvet cathode with  $D_1=6$  cm or 7 cm has not been changed by a strip reflector. This phenomenon is odd at first.

**Table 4: Frequency list for geometries with a strip reflector, showing the microwave frequencies based on their relative power for different geometries.**

Cathode width (cm)	D1 (cm)	D2 (cm)	Dominant peak (GHz)	Secondary Peak (GHz)
3.5	4	3.08	2.0	3.16
3.5	4	4.08	2.0	3.95
3.5	4	5.08	1.91	3.80
3.5	4	6.08	1.92	3.80
3.5	5.08	3	2.0	2.90
3.5	5.08	4	1.95	3.90
3.5	5.08	5	1.93	3.86
3.5	5.08	6	1.95	3.90
3.5	6	2.08	2.70	2.0
3.5	6	3.08	2.70	2.0
3.5	6	4.08	2.75	2.0
3.5	6	5.08	2.70	2.0
3.5	6	6.08	2.70	2.0
3.5	7	3.08	2.69	-
3.5	7	4.08	2.69	-
1	4	3	2.70	2.95
1	4	4	1.64	3.05
1	4	5	1.64	3.10
1	4	6	2.95	1.60
1	5	3	1.90	3.0
1	5	4	1.90	3.0
1	5	5	1.90	3.80
1	5	6	1.84	3.70
1	6	3	2.85	-
1	6	4	1.90	3.80
1	6	5	3.68	1.82
1	6	6	1.80	3.60

For the 1 cm velvet emitter, the strip reflector changes the dominant microwave frequencies too, although these changes are not as neat as for the 3.5 cm velvet emitter. We do observe that the microwave power generally is increased by the strip reflector. We notice that the microwave frequencies for a 1 cm velvet cathode are slightly lower than those for a 3.5 cm velvet cathode, with a similar diode structure. A reason for this is that we measure the cathode position from its middle point to the back wall of the cathode. Although the D1 is of the same value both for the 1 cm and 3.5 cm velvet cathode, the actual E-beam edge position for the 1 cm velvet cathode is different from that for the 3.5 cm cathode. This difference leads to different cavity sizes. This different frequency proves that the cavity formation in the diode region depends on the E-beam positions. Another phenomenon is that the frequencies which are way off of our expectation for the 1 cm velvet cathode occur more often than for the 3.5 cm velvet cathode. One possible reason is that the E-beam has a smaller width for the 1 cm velvet cathode. The reflection effect for narrower E-beam as a conductor may not be as strong as from an E-beam with a greater thickness.

Reviewing the frequency lists in table 2, 3 and 4, we find that different microwave frequencies exist simultaneously for the same diode structure without reflectors, with a donut reflector and with a strip reflector. Different reflector sets just change the microwave power or shift a dominant peak frequency to the secondary peak frequency. That is, different reflector sets enhance one microwave frequency and suppress another one.

Another important phenomenon we observe is that the microwave frequencies are almost independent of the reflector position. The reflector at different positions should lead to different microwave reflection intensities. This means that the microwave reflection by the reflector is not as



strong as that by the E-beam. The microwave frequency is still determined by the virtual cavity mentioned above. This phenomenon was out not expected.

The different performance of the donut and strip reflector has to be explained. We might be able to explain the different effects of the donut and the strip reflector by their different microwave reflection intensities. However, it has also been observed that the reflector positions have little influence on the microwave frequencies. This result reduces the strength of the argument for different microwave reflection intensities.

Another important phenomenon is that the middle part of the strip reflector has an obvious damaged spot after a lot of shots. If this damaged spot is caused by the microwave reflection, the spot should fade away gradually along the radial direction, which is not the case. We understand that a large fraction of the electrons collected in the virtual cathode move along the waveguide. We believe that the damaged spot is caused by those escaping electrons. In this way, we consider the strip reflector as an electron collector. This electron collection can change the field structure in the diode region, leading to a propagating mode shift.

Another phenomenon worth mentioning is that the dominant peak frequencies are in some cases half or double the secondary peak frequencies. We believe that this is a harmonic.

## **VI. Summary**

Given the above analysis, we can conclude that the E-beam plays an important part in forming a cavity in the geometries illustrated in Fig. 3. The donut reflector has little influence on the microwave frequency and the strip reflector has an obvious effect on the microwave frequency. Although the reflectors must reflect the microwaves, we believe that collecting electrons has an important effect on the field structure in the diode region.

We understand that the virtual cathode oscillates in a certain frequency range, which primarily depends on the gap distance of the diode and the applied voltage. Microwaves with that frequency range are produced by the vircator. Once a cavity forms in the diode region, microwaves of a certain frequency in this range are enhanced by resonance and non-resonant frequencies are suppressed. The frequency enhanced by resonance becomes the dominant peak. Because different mode resonant frequencies of a cavity sometimes coincide, different modes may propagate in the waveguide simultaneously, which makes the mode measurement more complicated.